Dynamics of magnetization growth and relaxation in ferrofluids

Igor M. Subbotin [*] and Alexey O. Ivanov [†]
Department of Theoretical and Mathematical Physics, Ural Mathematical Center, Ural Federal University, 51 Lenin Avenue, Ekaterinburg 620000, Russia

Philip J. Camp [‡]
School of Chemistry, University of Edinburgh, David Brewster Road, Edinburgh EH9 3FJ, Scotland

(Received 21 June 2024; accepted 6 August 2024; published 27 August 2024)

The dynamics of the growth and relaxation of the magnetization in ferrofluids are determined using theory based on the Fokker-Planck-Brown equation, and Brownian-dynamics simulations. Magnetization growth starting from an equilibrium nonmagnetized state in zero field, and following an instantaneous application of a uniform field of arbitrary strength, is studied with and without interparticle interactions. Similarly, magnetization relaxation is studied starting from an equilibrium magnetized state in a field of arbitrary strength, and following instantaneous removal of the field. In all cases, the dynamics are studied in terms of the time-dependent magnetization $m(t)$. The field strength is described by the Langevin parameter α, the strength of the interparticle interactions is described by the Langevin susceptibility χ_L, and the individual particles undergo Brownian rotation with time τ_B. For noninteracting particles, the average growth time decreases with increasing α due to the torque exerted by the field, while the average relaxation time stays constant at τ_B; with vanishingly weak fields, the timescales coincide. The same basic picture emerges for interacting particles, but the weak-field timescales are larger due to collective particle motions, and the average relaxation time exhibits a weak, nonmonotonic field dependence. A comparison between theoretical and simulation results is excellent for noninteracting particles. For interacting particles with $\chi_L = 1$ and 2, theory and simulations are in qualitative agreement, but there are quantitative deviations, particularly in the weak-field regime, for reasons that are connected with the description of interactions using effective fields.

DOI: 10.1103/PhysRevE.110.024610

I. INTRODUCTION

Ferrofluids are colloidal suspensions of ferromagnetic or ferrimagnetic nanoparticles in a nonmagnetic carrier liquid [1]. If the particles are not too large, then each one can be considered as a single, homogeneously magnetized grain. Further, if the particles are spherical, then the interactions between them are equivalent to those between point magnetic dipoles [2]. Many properties of ferrofluids can be understood in terms of the interactions between particles, and the aligning effect of an applied magnetic field. For example, the magnetoviscous effect is an increase in the suspension viscosity on application of a field, and it arises from the formation of chains of particles aligned with the field [3]. The optical properties of ferrofluids are also controlled by the structural organization of the constituent particles, which depends on the applied field [4]. Important material properties of a ferrofluid include its magnetization curve and initial magnetic susceptibility (static or dynamic). The dynamic initial magnetic susceptibility $\chi(\omega)$ describes how the magnetization of a ferrofluid responds to a weak ac magnetic field with given angular frequency ω. Based on the fluctuation-dissipation theorem and linear-response theory, features in $\chi(\omega)$ can be connected with characteristic timescales for equilibrium particle motions within the ferrofluid [5]. The dynamics of ferrofluids in strong fields are beyond the linear-response regime, and so these need to be considered separately [6]. A widely studied example of such dynamics is magnetic relaxation, where the ferrofluid is magnetized in a strong magnetic field, the system is allowed to equilibrate, and then the field is turned off. The decay of the magnetization is monitored to gain insights on nanoparticle dynamics. The analytical technique of magnetorelaxometry [7,8] can be used for characterization of the magnetic nanoparticles themselves [9], as a probe of local rheology [10], and in biomedical imaging [11–13].

Herein, the discussion is limited to the case of Brownian rotation of the magnetic nanoparticles. In this case, all types of magnetization dynamics are a result of body rotations of the particles, which are affected by particle size, carrier-liquid viscosity, temperature, interparticle interactions, and other fields [5,14–19]. Néel rotation [1] is not considered here, although

*Contact author: igor.subbotin@urfu.ru
†Contact author: alexey.ivanov@urfu.ru
‡Contact author: philip.camp@ed.ac.uk

some interesting effects are to be anticipated in the collective dynamics [20–24].

The primary focus of this work is the dynamics of magnetization growth, this being what happens when a ferrofluid is at equilibrium in zero field, and then a field of arbitrary strength is switched on instantaneously. This case has been studied much less than the opposite one of magnetic relaxation. In what follows, growth refers to when a field is turned on, and relaxation refers to when a field is turned off. Growth dynamics in suspensions of noninteracting magnetic nanoparticles were studied by Yoshida and Enpuku [25] by numerical solution of the Fokker-Planck-Brown (FPB) equation describing the one-particle orientational distribution function [26–28]. Characteristic timescales describing the magnetization growth were computed for various field strengths defined by the Langevin parameter α that compares the strength of the field-particle Zeeman interaction to the thermal energy. The timescales decrease with increasing α as a result of the increased torque on each particle dipole moment. This has been observed experimentally, for example, in suspensions of magnetotactic bacteria [29].

One of the aims of the present study is to determine the effects of interparticle interactions on the rate of magnetization growth. This is done using both theory (with the FPB equation) and Brownian-dynamics (BD) simulations. The theoretical approach is similar to that taken in the study of magnetization relaxation, in that the effects of interactions are described in terms of an effective field experienced by any one particle. Related modified mean-field (MMF) theories have been shown to be highly successful in describing both the static and dynamic properties of ferrofluids [30,31].

Another aim of the work is to complete the description of magnetic relaxation by considering weak fields; so far, studies have been focused on the case of strong aligning fields [17,19]. It is important to complete this analysis, because in the weak-field limit—corresponding to the linear-response regime—the timescales describing relaxation and growth should coincide. In fact, the analysis is a quite simple extension of the approach described in Ref. [17], and so only brief details are required here.

To summarize, the main outcomes from this study are the relaxation and growth timescales as functions of α, and descriptions of how they are affected by interparticle interactions. The growth timescale decreases rapidly with increasing α, as the field-particle interactions overcome the particle-particle interactions. The relaxation timescale is only weakly dependent on α, and as anticipated, it coincides with the growth timescale with small values of α. In general, all timescales increase with increasing interaction strength due to the spatial and orientational correlations between particles leading to collective motions. While such increases have been seen before in different situations, including the ac response in the linear and nonlinear regimes [21,32–34], and relaxation from the fully magnetized state [17], the effects of interactions on the growth and relaxation dynamics with arbitrary field strengths have not yet been analyzed in detail.

The rest of this article is organized as follows. The model and methods are described in Sec. II, including all theoretical and simulation aspects. The results are presented in Sec. III, which is organized in terms of noninteracting particles (Sec. III A) and interacting particles (Sec. III B). Section IV concludes the article.

II. MODEL AND METHODS

The system is modeled as a suspension of N spherical ferromagnetic particles, each with diameter σ, in a liquid with viscosity η at temperature T. The total volume of the suspension is V. If the particles are homogeneously magnetized, then the net magnetic interaction between two different particles is the same as that between two point dipoles [2]; the dipole moment on particle i is denoted by the vector $\boldsymbol{\mu}_i$, and the magnitude of the dipole moment $\mu = |\boldsymbol{\mu}_i|$ is the same for each particle. The potential energy of the system in an applied magnetic field $\boldsymbol{H}$ is

$$U = \sum_{i=1}^{N}\sum_{j>i}^{N}[u_s(i,j) + u_d(i,j)] - \mu_0\sum_{i=1}^{N}(\boldsymbol{\mu}_i\cdot\boldsymbol{H}), \quad (1)$$

where u_s is a short-range isotropic potential, u_d is the anisotropic dipole-dipole potential, and μ_0 is the vacuum permeability. The short-range potential u_s is chosen for mathematical convenience: for theory, the hard-sphere potential is the simplest; for simulations, a continuous repulsive potential is easiest, and this will be defined in Sec. II B. The dipolar interaction is

$$u_d(i,j) = \frac{\mu_0}{4\pi}\left[\frac{(\boldsymbol{\mu}_i\cdot\boldsymbol{\mu}_j)}{r_{ij}^3} - \frac{3(\boldsymbol{\mu}_i\cdot\boldsymbol{r}_{ij})(\boldsymbol{\mu}_j\cdot\boldsymbol{r}_{ij})}{r_{ij}^5}\right], \quad (2)$$

where $\boldsymbol{r}_{ij} = \boldsymbol{r}_j - \boldsymbol{r}_i$ is the separation vector between the particle centers, and $r_{ij} = |\boldsymbol{r}_{ij}|$. There are several key parameters that characterize the system. The number concentration is $\rho = N/V$, the particle volume is $v = \pi\sigma^3/6$, and the volume fraction of the particles is therefore

$$\varphi = \rho v = \frac{N\pi\sigma^3}{6V}. \quad (3)$$

The strength of the interactions between the particles is measured with the dipolar coupling constant, defined by

$$\lambda = \frac{\mu_0\mu^2}{4\pi\sigma^3 k_B T}. \quad (4)$$

The initial magnetic susceptibility of noninteracting particles is equal to the Langevin value

$$\chi_L = \frac{\rho\mu_0\mu^2}{3k_B T} = 8\varphi\lambda, \quad (5)$$

and the presence of interactions increases the static susceptibility in a known way; the leading-order correction to the susceptibility gives $\chi = \chi_L(1 + \chi_L/3)$ [35]. The strength of the particle-field interaction is given by the Langevin parameter

$$\alpha = \frac{\mu_0\mu H}{k_B T}. \quad (6)$$

The single-particle dynamics are described by the Brownian rotation time

$$\tau_B = \frac{\pi\eta\sigma^3}{2k_B T}. \quad (7)$$

The magnetization of a system at time t is defined by

$$\boldsymbol{M}(t) = \frac{1}{V}\sum_{i=1}^{N}\boldsymbol{\mu}_i(t). \tag{8}$$

Apart from thermal fluctuations, $\boldsymbol{M}$ is aligned with the field $\boldsymbol{H}$, and so it is sufficient to consider a corresponding reduced scalar magnetization

$$m(t) = \frac{|\boldsymbol{M}(t)|}{\rho\mu}, \tag{9}$$

where $\rho\mu$ is the saturation magnetization, and $0 \leqslant m(t) \leqslant 1$.

A. Theory

The general theoretical approach is to solve the FPB equation [26–28] for the time-dependent, one-particle orientational distribution function (ODF) $W(t, z)$, where t is the time, and $z = \cos\theta$ represents the projection of the dipole moment of a particle with polar angle θ onto the field direction, taken to be the laboratory z axis. The key difference between growth and relaxation is reflected in the boundary conditions for solving the FPB equation: in growth, $m(t \leqslant 0) = 0$, the field is turned on, and $m(\infty)$ reaches the equilibrium magnetization; in relaxation, $m(t \leqslant 0) > 0$, the field is turned off, and the system reaches the equilibrium state of zero magnetization [$m(\infty) = 0$]. The solution of the FPB equation for relaxation starting from an infinite aligning field [$m(t \leqslant 0) = 1$] has been described in detail in earlier publications [17,19]. The solution of the FPB equation in the case of weak, perturbing, ac fields has also been carried out [14–16], and because of the fluctuation-dissipation theorem [18], the characteristic timescales in the dynamic magnetic susceptibility are also those that control the response to switching on or off weak fields. The nonlinear response of the magnetization to a strong ac field has also been studied, including the effects of interactions through the introduction of an effective local field [21,33,34].

The organization of this part of the article is as follows: Sec. II A 1—magnetization growth of noninteracting particles; Sec. II A 2—analytical approximation to the magnetization growth of noninteracting particles; Sec. II A 3—magnetization growth of interacting particles; and Sec. II A 4—magnetization relaxation of interacting particles.

1. Magnetization growth: Noninteracting particles

The FPB equation for an isolated particle i in an applied magnetic field is [26–28]

$$2\tau_B\frac{\partial W_0}{\partial t} = \frac{\partial}{\partial z_i}\left[\left(1 - z_i^2\right)\left(\frac{\partial W_0}{\partial z_i} - \alpha W_0\right)\right], \tag{10}$$

where τ_B is the Brownian rotation time, $z_i = \cos\theta_i$, and $W_0 \equiv W_0(t, z_i)$ is the one-particle ODF. The subscript "0" in W_0 signifies the ideal, noninteracting case, as this specific function will be required later when including interactions. W_0 is normalized, and it determines the reduced magnetization $m(t)$:

$$\frac{1}{2}\int_{-1}^{1} W_0(t, z_i)dz_i = 1, \tag{11a}$$

$$\frac{1}{2}\int_{-1}^{1} W_0(t, z_i)z_i dz_i = m(t). \tag{11b}$$

The initial condition for the problem (10) is the fully demagnetized state, i.e., $m(0) = 0$ and $W_0(0, z_i) = 1$. The FPB equation therefore describes the evolution of the probability density from the uniform orientation distribution to the equilibrium one, which is established at infinite time:

$$W_0(\infty, z_i) = \left(\frac{\alpha}{\sinh\alpha}\right)\exp(\alpha z_i), \tag{12a}$$

$$m(\infty) = \coth\alpha - \frac{1}{\alpha} \equiv L(\alpha). \tag{12b}$$

This solution follows from the FPB equation (10) with the stationarity condition $(\partial W_0/\partial t) = 0$; the Langevin function $L(\alpha)$ describes the equilibrium magnetization of an ensemble of noninteracting magnetic particles.

The common approach to the solution of Eq. (10) is based on an expansion of the ODF in terms of Legendre polynomials $P_k(z)$ [36],

$$W_0(t, z_i) = \sum_{k=0}^{\infty} A_k(t)P_k(z_i), \tag{13}$$

where $A_k(t)$ is the time-dependent amplitude of the kth harmonic. Evidently, the magnetization is defined by the first harmonic, $m(t) = A_1(t)/3$. Using expansion (13), Eq. (10) is transformed into an infinite set of ordinary differential equations for the amplitudes with $k \geqslant 1$:

$$\frac{2\tau_B}{k(k+1)}\frac{dA_k}{dt} + A_k = \alpha\left(\frac{A_{k-1}}{2k-1} - \frac{A_{k+1}}{2k+3}\right). \tag{14}$$

The initial conditions are $A_0(t) = 1$ and $A_k(0) = 0$ $(k \geqslant 1)$. Obviously, this set of equations can only be solved for a finite number of equations K, the value of which is chosen to provide a desired accuracy. Some general comments on the behavior of $m(t)$ at short, intermediate, and long times are as follows.

The initial rise of the magnetization curve is given by the simple expression

$$m(t \to 0) \approx m(0) + \frac{t}{3}\left(\frac{dA_1}{dt}\right)_{t=0} = \frac{\alpha}{3}\frac{t}{\tau_B}, \tag{15}$$

and so it is controlled by both the individual Brownian time τ_B and the dimensionless magnetic field strength α, which provides the "driving force" of the magnetization dynamics.

The complete solution is expressed as a sum of exponential functions [37]:

$$m(t) = C_0 + \sum_{k=1}^{K} C_k\exp(\gamma_k t/\tau_B). \tag{16}$$

From the initial condition $m(0) = 0$, and matching the first derivatives of Eqs. (15) and (16), the coefficients must satisfy the following rules:

$$C_0 + \sum_{k=1}^{K} C_k = 0, \tag{17a}$$

$$\sum_{k=1}^{K} C_k \gamma_k = \frac{\alpha}{3}. \tag{17b}$$

For $m(t)$ to be finite, the values of γ_k must all be negative. Hence, by taking the long-time limit, the equilibrium magnetization is $m(\infty) = C_0 = A_1(\infty)/3$. At equilibrium, when $dA_k/dt = 0$, the complete set of coefficients A_k satisfies the equations

$$A_k = \alpha\left(\frac{A_{k-1}}{2k-1} - \frac{A_{k+1}}{2k+3}\right), \tag{18}$$

which follows from Eq. (14). It is emphasized that the solutions all depend on the number of equations K. In the long-time limit, the first amplitude approaches the value $A_1 = 3L(\alpha)$ as $K \to \infty$, and hence the magnetization $m(\infty)$ approaches the expected Langevin value (12b).

The parameters γ_k are equal to the roots of the determinant of a $K \times K$ matrix:

$$\begin{Vmatrix} -1-\gamma & -\frac{\alpha}{5} & 0 & 0 & 0 & \dots & 0 & 0 & 0 \\ \alpha & -3-\gamma & -\frac{3\alpha}{7} & 0 & 0 & \dots & 0 & 0 & 0 \\ 0 & \frac{6\alpha}{5} & -6-\gamma & -\frac{2\alpha}{3} & 0 & \dots & 0 & 0 & 0 \\ \vdots & \vdots & \vdots & \vdots & \vdots & \ddots & \vdots & \vdots & \vdots \\ 0 & 0 & 0 & 0 & \dots & 0 & \frac{K(K-1)\alpha}{2(2K-3)} & -\frac{K(K-1)}{2}-\gamma & \frac{K(K-1)\alpha}{2(2K+1)} \\ 0 & 0 & 0 & 0 & \dots & 0 & 0 & \frac{K(K+1)\alpha}{2(2K-1)} & -\frac{K(K+1)}{2}-\gamma \end{Vmatrix} = 0. \tag{19}$$

An important feature is that all K roots γ_k are real and negative. Hence, they can be put in descending order $0 > \gamma_1 > \gamma_2 > \ldots > \gamma_K$, the exponential functions in Eq. (16) are all decreasing functions of time, and $\exp(\gamma_1 t/\tau_B)$ decreases slowest.

In general, γ_k and the corresponding coefficients C_k can only be calculated numerically, and once more, all values depend on the truncation level K. Figure 1 shows the convergence of the longest timescale γ_1 with increasing K. Figure 1(a) shows the value of γ_1 as a function of K, and the results indicate that $K = 30$ is sufficient to achieve full convergence even at high values of α. Moreover, the higher the value of α, the more negative the value of γ_1, and hence the faster the growth rate. Figure 1(b) shows the value of K required to achieve convergence within a tolerance of 1 part in 10^3. Something like $K = 30$–40 is enough to give sufficiently well converged results with $\alpha \leqslant 50$.

The magnetization dynamics described by Eq. (16) are controlled by various characteristic timescales, which can be conveniently described with the help of an effective, instantaneous time $\tau(t)$. If at any time t

$$m(t) = m(\infty)\left\{1 - \exp\left[-\frac{t}{\tau(t)}\right]\right\}, \tag{20}$$

then

$$\tau(t) = -\left\{\frac{d}{dt}\ln\left[1 - \frac{m(t)}{m(\infty)}\right]\right\}^{-1}. \tag{21}$$

Substituting Eq. (16) into this expression gives

$$\frac{\tau(t)}{\tau_B} = -\frac{\sum_{k=1}^{K} C_k \exp(\gamma_k t/\tau_B)}{\sum_{k=1}^{K} \gamma_k C_k \exp(\gamma_k t/\tau_B)}. \tag{22}$$

Using Eq. (17) and $C_0 = m(\infty)$, the initial effective time is

$$\frac{\tau(0)}{\tau_B} = \frac{3m(\infty)}{\alpha}, \tag{23}$$

and hence at short times, from Eq. (20) with $t \to 0$,

$$m(t \to 0) \approx m(\infty)\left[\frac{t}{\tau(0)}\right] = \frac{\alpha}{3}\frac{t}{\tau_B}, \tag{24}$$

as per Eq. (15). It may be surprising that the initial effective time depends on the equilibrium value $m(\infty)$, but this arises naturally from the definition in Eq. (21), the expansion in Eq. (16), and the sum rules in Eq. (17). The effect is that in weak fields $\tau(0) \approx \tau_B$, and in strong fields $\tau(0) \approx 3/\alpha$.

At long times, the magnetization dynamics is controlled by the slowest-decaying exponential, and hence

$$\frac{\tau(\infty)}{\tau_B} \approx -\frac{1}{\gamma_1}. \tag{25}$$

Finally, an average growth time can be computed, which is more easily compared to the results from BD simulations:

$$\overline{\tau}(\text{on}) = \int_0^{\infty}\left[1 - \frac{m(t)}{m(\infty)}\right]dt. \tag{26}$$

With $m(t)$ given by Eq. (16), the result is

$$\frac{\overline{\tau}(\text{on})}{\tau_B} = \frac{1}{C_0}\sum_{k=1}^{K}\frac{C_k}{\gamma_k}. \tag{27}$$

2. *Magnetization growth: Noninteracting particles in the $K = 2$ approximation*

Although an accurate solution can only be obtained numerically, it is useful to illustrate the qualitative behavior by

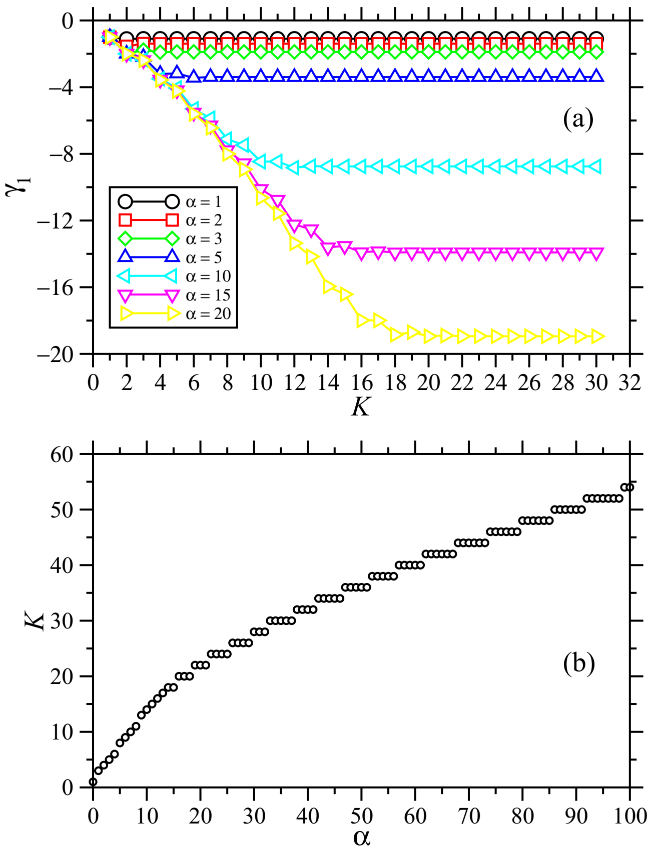

FIG. 1. (a) The root γ_1 as a function of the number of equations K with different Langevin parameters in the range $1 \leqslant \alpha \leqslant 20$. Symbols show the values calculated from Eq. (19), and the lines are guides to the eye. (b) The number of equations K required to reach convergence of γ_1 to within 0.1%.

solving the simple case with $K = 2$ analytically. The two roots γ_1 and γ_2 are given by

$$\gamma_1 = -2 + b, \tag{28a}$$

$$\gamma_2 = -2 - b, \tag{28b}$$

where $b = \sqrt{1 - \alpha^2/5}$. Hence, this analysis is restricted to small values of α, and certainly less than $\sqrt{5}$. The magnetization dynamics are given by

$$m(t) = \frac{\alpha}{4 - b^2} - \frac{\alpha(1+b)}{6b(2-b)} \exp\left[(-2+b)t/\tau_B\right] + \frac{\alpha(1-b)}{6b(2+b)} \exp\left[(-2-b)t/\tau_B\right]. \tag{29}$$

The equilibrium magnetization

$$m(\infty) = \frac{\alpha}{4 - b^2} = \frac{\alpha}{3 + \alpha^2/5} \tag{30}$$

is close to the exact value $L(\alpha)$ only for $\alpha \lesssim 2$. The instantaneous growth time is

$$\frac{\tau(t)}{\tau_B} = \frac{3b + (2 + b^2)\tanh(bt/\tau_B)}{(4 - b^2)[b + \tanh(bt/\tau_B)]}. \tag{31}$$

The initial growth time is

$$\frac{\tau(0)}{\tau_B} = \frac{3}{4 - b^2} = \frac{1}{1 + \alpha^2/15}, \tag{32}$$

which satisfies Eqs. (23) and (30). This function is approximately equal to the exact value $3L(\alpha)/\alpha$ with $\alpha \lesssim 2$. The longest growth time is

$$\frac{\tau(\infty)}{\tau_B} = -\frac{1}{\gamma_1} = \frac{1}{2 - b} = \frac{1}{2 - \sqrt{1 - \alpha^2/5}}. \tag{33}$$

Hence, the dynamics of magnetization growth are controlled by two characteristic timescales. At the beginning of the process, the growth time is given approximately by Eq. (32) and exactly by $3[L(\alpha)/\alpha]\tau_B$. With $K = 2$, the asymptotic growth time toward equilibrium is controlled by Eq. (33). With small values of α, $\tau(0)$ and $\tau(\infty)$ are both approximately equal to τ_B, and hence the growth time is approximately constant. As α increases, $\tau(\infty)$ decreases faster than $\tau(0)$, and so a crossover in timescales takes place during the magnetization process: the initial growth is slow, and the asymptotic growth is fast. At the $K = 2$ level of approximation, the average growth time is

$$\frac{\overline{\tau}(\text{on})}{\tau_B} = \frac{8 + b^2}{3(4 - b^2)} = \frac{3 - \alpha^2/15}{3 + \alpha^2/5}, \tag{34}$$

and this starts at 1, and is a decreasing function of α.

3. Magnetization growth: Interacting particles

For interacting particles the FPB equation can be written [31]

$$2\tau_B \frac{\partial W}{\partial t} = \frac{\partial}{\partial z_i}\left\{\left(1 - z_i^2\right)\left[\frac{\partial W}{\partial z_i} - \alpha W + W\frac{\partial u_{\text{eff}}(i)}{\partial z_i}\right]\right\}, \tag{35}$$

where $u_{\text{eff}}(i)$ is the effective interaction energy between particle i and all of the other $N - 1$ particles in the system. Each particle interacts with a total magnetic field composed of the external field $\boldsymbol{H}$ and an extra field $\boldsymbol{H}_{\text{MMF}}$ produced by all of the other particles in the system. Within the first-order MMF model [30], $u_{\text{eff}}(i)$ is approximated by an expression which is linear in the particle concentration ρ, and no spatial or orientational correlations between the particles are taken into account. Within this approximation,

$$u_{\text{eff}}(i) = -\frac{\mu_0(\boldsymbol{\mu}_i \cdot \boldsymbol{H}_{\text{MMF}})}{k_B T}, \tag{36}$$

with the effective field given by

$$\boldsymbol{H}_{\text{MMF}} = \frac{\rho}{4\pi}\int_{r\geqslant\sigma} d\boldsymbol{r}_{ij}\int d\boldsymbol{e}_j W_0(t, z_j) \times \left[\frac{3\boldsymbol{r}_{ij}(\boldsymbol{\mu}_j \cdot \boldsymbol{r}_{ij})}{r_{ij}^5} - \frac{\boldsymbol{\mu}_j}{r_{ij}^3}\right], \tag{37}$$

where $\boldsymbol{\mu}_j = \mu \boldsymbol{e}_j$. In this term, the integration over all possible positions and orientations of particle j is weighted by the ODF for noninteracting particles, i.e., W_0 from Eq. (10). Carrying out the integration gives

$$u_{\text{eff}}(i) = -\frac{\chi_L}{3} A_1 z_i, \tag{38}$$

and so Eq. (35) becomes

$$2\tau_B \frac{\partial W}{\partial t} = \frac{\partial}{\partial z_i}\left\{\left(1-z_i^2\right)\left[\frac{\partial W}{\partial z_i} - \alpha_{\rm eff}(t)W\right]\right\}, \quad (39)$$

with a time-dependent effective Langevin parameter

$$\alpha_{\rm eff}(t) = \alpha + \tfrac{1}{3}\chi_L A_1(t). \quad (40)$$

The equilibrium solution of this equation gives the well-known expression of the MMF static magnetization [30]:

$$\alpha_{\rm eff}(\infty) \equiv \alpha^*_{\rm eff} = \alpha + \chi_L L(\alpha), \quad (41a)$$

$$m(\infty) = L(\alpha^*_{\rm eff}). \quad (41b)$$

Turning to the time dependence, the one-particle ODF is written

$$W(t, z_i) = \sum_{k=0}^{\infty} B_k(t) P_k(z_i), \quad (42)$$

and the amplitudes B_k ($k \geqslant 1$) are determined by the set of ordinary differential equations

$$\frac{2\tau_B}{k(k+1)}\frac{dB_k}{dt} + B_k = \alpha_{\rm eff}(t)\left(\frac{B_{k-1}}{2k-1} - \frac{B_{k+1}}{2k+3}\right), \quad (43)$$

with the initial conditions $B_0(t) = 1$ and $B_k(0) = 0$ ($k \geqslant 1$). This set of equations is much more complicated than Eq. (14) because the coefficient $\alpha_{\rm eff}(t)$ is time-dependent, and so the general solution can only be found numerically. Since $A_1(0) = 0$ and $\alpha_{\rm eff}(0) = \alpha$,

$$m(t \to 0) \approx \frac{\alpha}{3}\frac{t}{\tau_B}. \quad (44)$$

This coincides with Eq. (15) for noninteracting particles, but the initial growth time is

$$\frac{\tau(0)}{\tau_B} = \frac{3m(\infty)}{\alpha}, \quad (45)$$

which is dependent not only on the applied field strength, but also on χ_L through $m(\infty)$ (41).

An analytical solution for interacting particles can be found only for very weak magnetizing fields, $\alpha \ll 1$. Here, only the first equations in the sets (14) and (43) are solved, giving

$$m(t) = \frac{\alpha}{3}\left[\left(1 + \frac{\chi_L}{3}\right)(1 - e^{-t/\tau_B}) - \frac{\chi_L}{3}\frac{t}{\tau_B}e^{-t/\tau_B}\right]. \quad (46)$$

The time-dependent growth time is

$$\frac{\tau(t)}{\tau_B} = 1 + \frac{\chi_L}{3 + \chi_L t/\tau_B}, \quad (47)$$

which decreases monotonically from $\tau(0) = (1 + \chi_L/3)\tau_B$ to $\tau(\infty) = \tau_B$. The average growth time is also independent of α:

$$\frac{\overline{\tau}(\text{on})}{\tau_B} = \frac{3 + 2\chi_L}{3 + \chi_L} \approx 1 + \frac{1}{3}\chi_L + \dots \quad (48)$$

These times are only independent of α because of the approximation of solving only for A_1 and B_1 ($K = 1$). The field dependence is manifested even for $K = 2$, as shown by the solution (31) for noninteracting particles, in which the growth time is determined to leading order (by symmetry) in α^2.

4. Magnetization relaxation: Interacting particles

The analysis of relaxation in Ref. [17] was restricted to the case of a completely magnetized initial state, i.e., $\alpha \to \infty$. The MMF approach can be extended straightforwardly to the case of finite α, and the result for the magnetization is

$$m(t) = \left\{L(\alpha^*_{\rm eff}) + \frac{1}{3}\chi_L L(\alpha) \times \left[\frac{t}{\tau_B} + \frac{1}{3}L_3(\alpha^*_{\rm eff})(e^{-3t/\tau_B} - 1)\right]\right\}e^{-t/\tau_B}, \quad (49)$$

where the function $L_3(z) = 1 - 3L(z)/z$. In general, $m(0) = L(\alpha^*_{\rm eff})$ as per the MMF magnetization curve [30]. When $\chi_L = 0$, $\alpha^*_{\rm eff} = \alpha$, and $m(t) = L(\alpha)\exp(-t/\tau_B)$, and so the Brownian rotation time is the only relevant timescale [17]. With a completely magnetized initial state, as studied in Ref. [17], $L(\infty) = L_3(\infty) = 1$, and so

$$m(t) = \left\{1 + \frac{\chi_L}{3}\left[\frac{t}{\tau_B} + \frac{1}{3}\left(e^{-3t/\tau_B} - 1\right)\right]\right\}e^{-t/\tau_B}. \quad (50)$$

The initial and asymptotic relaxation times are

$$\frac{\tau(0)}{\tau_B} = \frac{\alpha^*_{\rm eff}}{\alpha}, \quad (51a)$$

$$\frac{\tau(\infty)}{\tau_B} = 1. \quad (51b)$$

The MMF theory predicts that the relaxation time first increases, reaches a local maximum, and then decreases. For noninteracting particles, or for interacting particles in the strong-field limit, $\tau(0) = \tau_B$ [17]. That $\tau(\infty)$ does not depend on χ_L is an artifact of the MMF approximation; at least with a fully magnetized initial state, $\tau(\infty)$ is $(1 + \chi_L/3)\tau_B$ to leading order in χ_L [17]. The average relaxation time is defined by

$$\overline{\tau}(\text{off}) = \int_0^{\infty}\left[\frac{m(t)}{m(0)}\right]dt. \quad (52)$$

With the MMF result (49), this gives

$$\frac{\overline{\tau}(\text{off})}{\tau_B} = 1 + \frac{\chi_L L(\alpha)}{3L(\alpha^*_{\rm eff})}\left[1 - \frac{1}{4}L_3(\alpha^*_{\rm eff})\right]. \quad (53)$$

With small values of α, this approaches

$$\frac{\overline{\tau}(\text{off})}{\tau_B} = \frac{3 + 2\chi_L}{3 + \chi_L} \approx 1 + \frac{1}{3}\chi_L + \dots, \quad (54)$$

whereas in the strong-field limit, it approaches

$$\frac{\overline{\tau}(\text{off})}{\tau_B} \approx 1 + \frac{1}{4}\chi_L. \quad (55)$$

The behavior between these limits of α will be discussed below.

B. Brownian dynamics simulations

BD simulations were carried out using LAMMPS [38,39]. $N = 16^3 = 4096$ identical particles were simulated in all cases with the volume fraction equal to $\varphi = 0.125$, and the dipolar coupling constant equal to $\lambda = 1$ (with and without interactions) or $\lambda = 2$ (with interactions). The choices of φ and λ were arbitrary for the noninteracting system. These parameters give Langevin susceptibilities of $\chi_L = 1$ and 2, and are physically relevant for real ferrofluids. The simulation box was cubic, periodic boundary conditions were applied in all three directions, and the long-range dipolar interactions were handled using the particle-particle particle-mesh method with a relative error in the forces of 10^{-4}. A soft-core, short-range potential is most convenient for these calculations, and the Weeks-Chandler-Andersen [40] interaction with energy parameter ϵ and particle diameter σ was used here:

$$u_s(i,j) = \begin{cases} 4\epsilon\left[\left(\frac{\sigma}{r_{ij}}\right)^{12} - \left(\frac{\sigma}{r_{ij}}\right)^{6} + \frac{1}{4}\right] & r_{ij} \leqslant 2^{1/6}\sigma, \\ 0 & r_{ij} > 2^{1/6}\sigma. \end{cases} \tag{56}$$

The temperature was set equal to $T^* = k_B T/\epsilon = 1$. As explained in detail several times before [14,15], a Langevin thermostat with a large friction coefficient can be used to produce overdamped, and hence Brownian, dynamics. In Lennard-Jones units (indicated by $*$), the `damp` parameter in LAMMPS was set equal to 0.05, which results in a Brownian rotation time of $\tau_B^* = 1/6T^*\mathtt{damp} = 3.3333$ [14,15] and no discernible inertial motion.

Each system was first equilibrated with $\alpha = 0$ for $n_t = 2 \times 10^4$ time steps with $\delta t^* = 0.005$, corresponding to $t = 30\tau_B$. Then a field corresponding to the desired Langevin parameter α was switched on, and another n_t time steps were carried out to simulate the magnetization growth process. Finally, relaxation in zero field was simulated over n_t time steps. The value of n_t was chosen so that the magnetization fully equilibrated during each stage of the growth and relaxation processes. The growth-relaxation procedure was repeated 200 times for the noninteracting system, and 100 times for the interacting systems, and the magnetization for each type of process was averaged. Despite the averaging, it was not possible to get very reliable results for the instantaneous growth or relaxation times from the magnetization by direct numerical differentiation. Instead, and as noted in Sec. II A, it was more convenient to compare the theoretical and simulated average times, defined by Eq. (26) for growth and Eq. (52) for relaxation.

III. RESULTS

The simulation protocol is illustrated in Fig. 2(a), which shows the magnetization $m(t)$ during the equilibration stage ($t < 0$), followed by growth with $\alpha = 5$ ($0 \leqslant t < 30\tau_B$), and then relaxation ($30\tau_B \leqslant t \leqslant 60\tau_B$). The average results are shown in the figure. The equilibrium magnetization with the field on increases with increasing interaction strength due to the effective field felt by each particle being larger than the applied field. This is captured accurately by the first-order MMF theory (41). By eye, the initial growth rate in a strong field is not strongly affected by interactions, whereas the relaxation rate decreases with increasing interaction strength [17–19].

The equilibrium magnetization curves are shown in Fig. 2(b). The BD simulations results for noninteracting particles of course agree with the exact formula. The first-order MMF theory which accounts for interactions (41) is in excellent agreement with the BD simulation results.

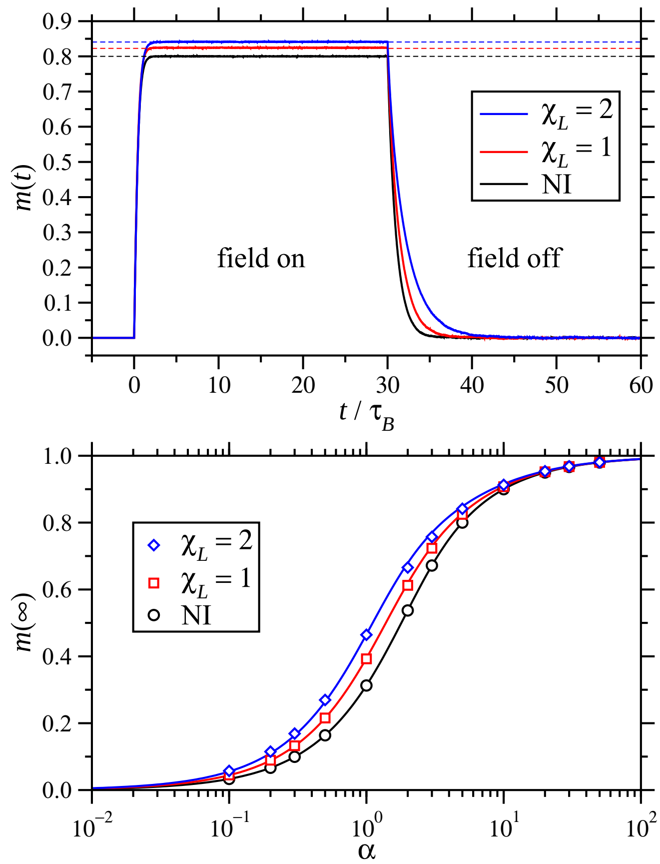

FIG. 2. (a) BD simulation results for systems with $\varphi = 0.125$ and $\alpha = 5$ illustrating the growth and relaxation processes. Each stage lasts for $30\tau_B$. The dashed lines show the predictions from first-order MMF theory (41). (b) Magnetization curves from BD simulations (points) and MMF theory (41) (lines). NI means the noninteracting system.

A. Magnetization growth and relaxation of noninteracting particles

The growth of the magnetization with noninteracting particles is illustrated in Fig. 3(a) for Langevin parameters $\alpha = 0.5, 1, 2, 3, 5$, and 10. The BD simulation results are compared with the theoretical predictions from Eq. (16) with $K = 30$ (numerical), and from Eq. (29) with $K = 2$ (analytical) for $\alpha \leqslant 2$ only. On that scale, the analytical $K = 2$ result is hardly distinguishable from the numerical results with $K = 30$, which can be considered practically exact.

The results are shown on a linear-log plot in Fig. 3(b). The quantity $1 - m(t)/m(\infty)$ is plotted on the y axis, and its roughly straight-line behavior at long times indicates an asymptotic quasi-exponential decay controlled by γ_1. At short times, the decay is less rapid but increases with α according to Eq. (15). The agreement between the BD simulations and the numerical evaluation of the theory is excellent, as expected. The $K = 2$ approximation is already quite poor with $\alpha = 2$.

To illustrate the changes in growth rate during the growth process, the instantaneous time $\tau(t)$ (21) from the FPB theory for noninteracting particles is plotted in Fig. 4; the same results are shown in Figs. 4(a) and 4(b) for subsequent comparison with results for interacting particles. With very small

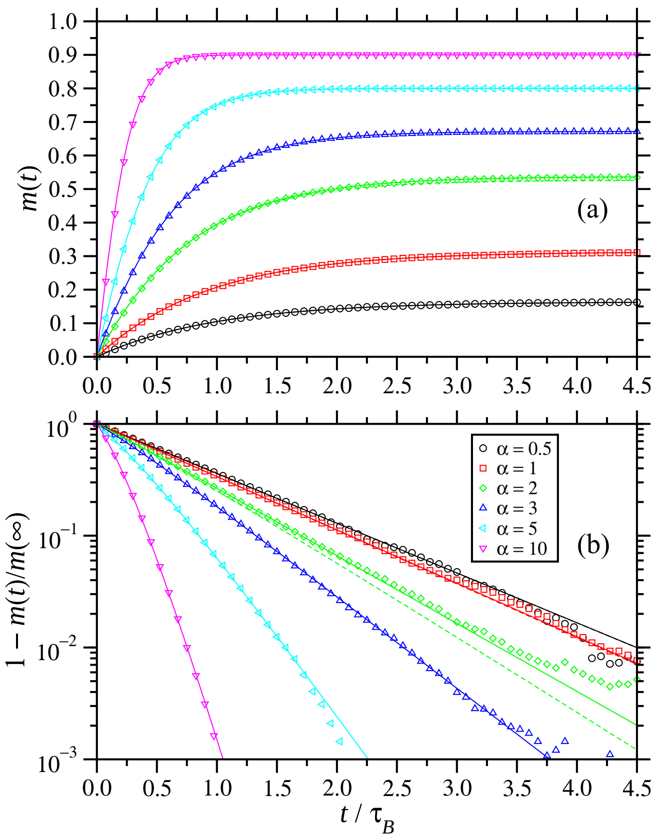

FIG. 3. (a) Magnetization growth in systems of noninteracting particles with various values of α. The points are from BD simulations, the solid lines are from Eq. (16) with $K = 30$ (numerical), and the dashed lines for $\alpha \leqslant 2$ are from Eq. (29) with $K = 2$ (analytical). (b) The function $1 - m(t)/m(\infty)$ from the same data sets as in panel (a). The meanings of the points and lines are the same in panels (a) and (b). For clarity, only every 10th point of the simulation results is shown.

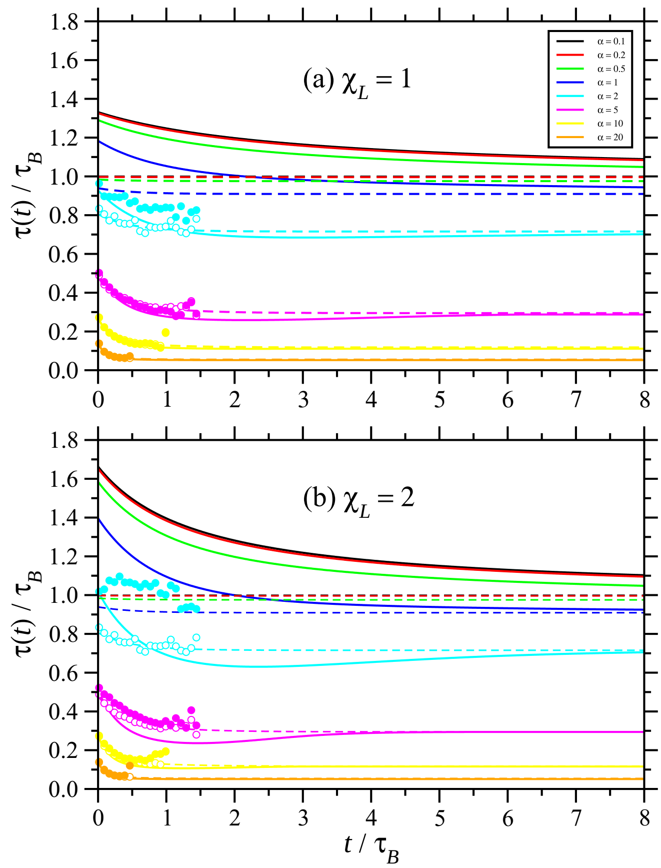

FIG. 4. The instantaneous growth time in systems with various values of α and (a) $\chi_L = 1$ and (b) $\chi_L = 2$. Theoretical predictions are shown for interacting systems (solid lines) and noninteracting systems (dashed lines). BD simulation results for large values of α and at short times are shown for interacting systems (filled points) and noninteracting systems (unfilled points); for clarity, only every 10th point of the simulation results is shown.

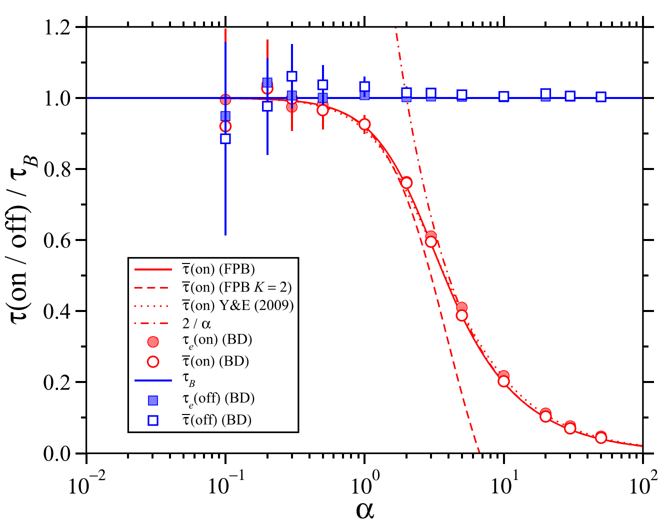

FIG. 5. The average relaxation and growth times as functions of α for the noninteracting system. The unfilled points are given by Eqs. (26) and (52) using BD simulation results, the lines are the corresponding results from theory, and the filled points are $1/e$ times from BD simulations. Y&E (2009) refers to the work of Yoshida and Enpuku [25].

values of α, $\tau(t)$ is very close to τ_B. With increasing α, there is a more pronounced decrease in $\tau(t)$ before leveling off at a value much less than τ_B. This is consistent with the comments made in Sec. II A 2 in the framework of the $K = 2$ solution.

Also shown in Fig. 4 are some BD simulation results for $\tau(t)$ with large values of α and at short times. The results with small values of α and/or at long times are too noisy, with the scatter along the whole y axis. With small values of α, the statistical fluctuations in $m(t)$ are significant, and these are magnified when trying to extract $\tau(t)$ as an instantaneous numerical derivative from Eq. (21). Similarly, at long times, the term in square brackets in Eq. (21) is very small, and the statistical noise in $\tau(t)$ obscures the results. Nonetheless, the limited BD simulation results are in good agreement with the theoretical predictions.

The average growth time is shown in Fig. 5. This was estimated from the BD simulation results in two different ways: from the integral in Eq. (26); and as the time $\tau_e(\text{on})$ it takes for $1 - m(t)/m(\infty)$ to reach $1/e$. The error bars are the statistical uncertainties estimated from the 200 repeats. First, there is very little difference between $\overline{\tau}(\text{on})$ and $\tau_e(\text{on})$. Second, both parameters decrease with increasing Langevin parameter α and hence the torque acting on the dipoles. The BD simulation results with $\alpha = 0.1$ show some scatter and have large error bars because the statistical fluctuations are significant as compared to the small values of $m(t)$ in Eq. (26). With $\alpha \geqslant 0.2$ the simulation results are adequate.

Figure 5 also shows the theoretical results with $K = 30$ and $K = 2$, and an expression determined by Yoshida and Enpuku by fitting an *ad hoc* function to the growth time from a numerical solution of the FPB equation [25]:

$$\frac{\overline{\tau}(\text{on})}{\tau_B} = \frac{1}{\sqrt{1 + 0.21\alpha^2}}. \tag{57}$$

The $K = 2$ approximation is only valid for $\alpha \lesssim 2$, whereas the $K = 30$ results, and the Yoshida and Enpuku expression, are in excellent agreement with the BD simulation results. The asymptotic behavior with large values of α appears to be similar to $2/\alpha$, which is also shown in Fig. 5. The *equilibrium* relaxation time of magnetization fluctuations parallel to a static field is [41,42]

$$\frac{\tau_\parallel}{\tau_B} = \frac{\alpha L_1(\alpha)}{L(\alpha)}, \tag{58}$$

where $L_1(\alpha) = dL/d\alpha$. With large values of α, this approaches $1/\alpha$. Apart from the constant of proportionality, the growth time in strong fields is the same.

The average relaxation time from BD simulations and theory is also shown in Fig. 5. These results confirm that for noninteracting particles, there is only one relaxation time equal to τ_B, and this is independent of α. This is because the relaxation mechanism in zero field (when switched off) is purely Brownian, and with no additional torques arising from the coupling between the particles. As before, the BD simulation results with $\alpha = 0.1$ are too noisy, but with $\alpha \geqslant 0.2$, they are adequate. The integral time $\overline{\tau}(\text{off})$ (52) and $1/e$ time $\tau_e(\text{off})$ are in good agreement with one another.

Finally, the comparison between $\overline{\tau}(\text{on})$ and $\overline{\tau}(\text{off})$ confirms that with small values of α, there is only one characteristic timescale, equal to τ_B. The growth time of the magnetization in a weak field is the same as the relaxation time of a small magnetization.

B. Magnetization growth and relaxation of interacting particles

From here on, "the theory" refers only to the numerical solutions of the FPB equation with interactions described at the first-order MMF level. The magnetization growth in systems of interacting particles with $\chi_L = 1$ is shown in Fig. 6. With small and large values of α, the agreement between the theory and BD simulations is good. With intermediate values of $\alpha = 1$–5, there are clear deviations between them at times in the region of $t \simeq \tau_B$; the theory predicts more rapid growth.

This discrepancy is reflected in the instantaneous growth times $\tau(t)$ shown in Fig. 4(a). The theory correctly predicts that the initial growth times are larger in the presence of interactions (45), but the available simulation results for $\alpha = 2$ show that the theory underestimates the value. In stronger fields, the results for interacting and noninteracting particles coincide, because the field-particle interaction dominates the particle-particle interaction. The theory also predicts some interesting nonmonotonic behavior for intermediate values of α, with the growth time dipping below that for noninteracting particles, before rising again and converging. This particular prediction could be an artifact of the MMF approach, as similar unusual behavior is predicted for the relaxation dynamics [17].

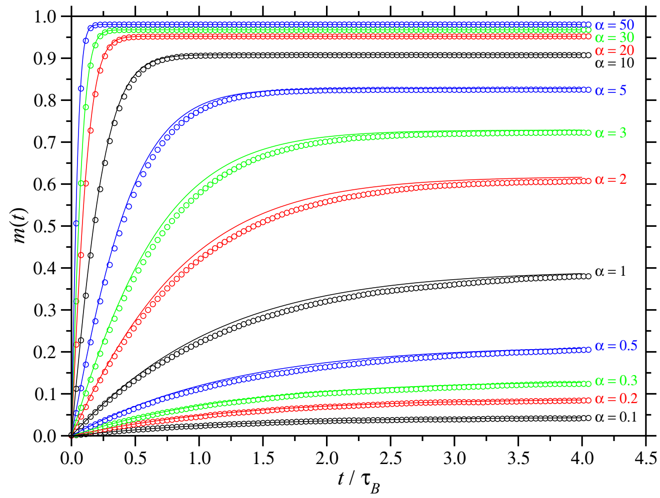

FIG. 6. Magnetization growth in systems of interacting particles with $\varphi = 0.125$, $\lambda = 1$, $\chi_L = 1$, and various values of α. The lines are from the FPB theory, and the points are from BD simulations. For clarity, only every 5th point of the simulation results is shown.

The average growth and relaxation times are shown in Fig. 7. As before, BD simulations results for both $\overline{\tau}$ and τ_e are shown, and these are in good agreement. $\overline{\tau}(\text{on})$ is significantly larger than τ_B in weak fields, but then decreases with increasing α. $\overline{\tau}(\text{off})$ is close to $\overline{\tau}(\text{on})$ in weak fields, and seems to show a weak maximum with increasing α, before approaching its initial value. The theory at the MMF level predicts the low-α average times to be $5\tau_\text{B}/4$ [Eqs. (48) and

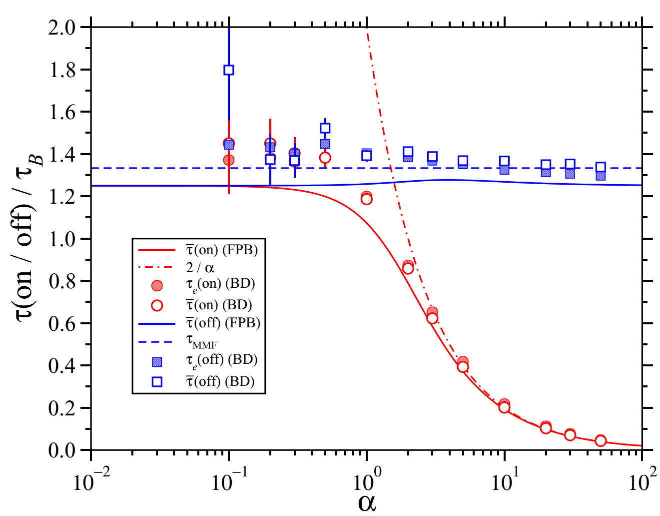

FIG. 7. The average relaxation and growth times as functions of α for the system with $\varphi = 0.125$ and $\lambda = 1$ ($\chi_L = 1$). The unfilled points are given by Eqs. (26) and (52) using BD simulation results, the lines are the corresponding results from theory, and the filled points are $1/e$ times from BD simulations.

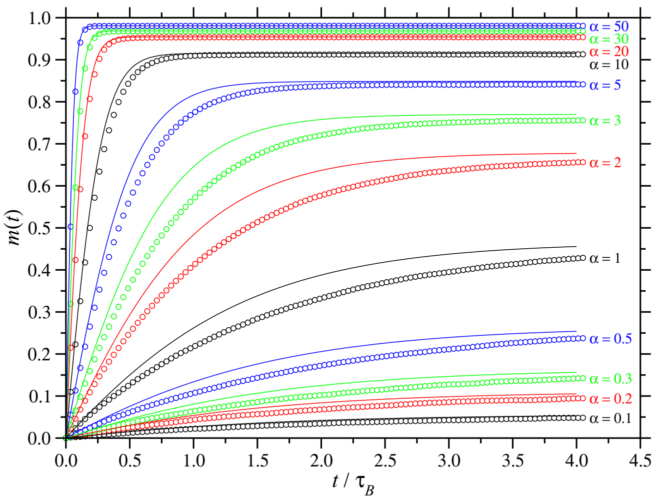

FIG. 8. Magnetization growth in systems of interacting particles with $\varphi = 0.125$, $\lambda = 2$, $\chi_L = 2$, and various values of α. The lines are from the FPB theory, and the points are from BD simulations. For clarity, only every 5th point of the simulation results is shown.

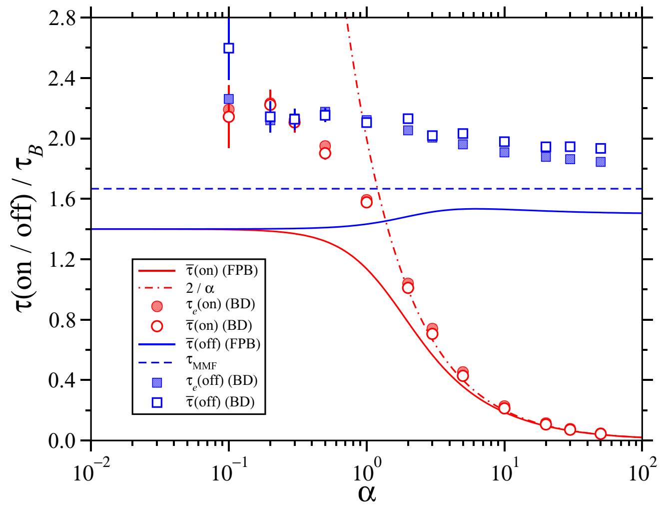

FIG. 9. The average relaxation and growth times as functions of α for the system with $\varphi = 0.125$ and $\lambda = 2$ ($\chi_L = 2$). The unfilled points are given by Eqs. (26) and (52) using BD simulation results, the lines are the corresponding results from theory, and the filled points are $1/e$ times from BD simulations.

(54)], which is smaller than the apparent simulation values. In fact, the simulation results are closer to $(1 + \chi_L/3)\tau_B$, labeled as τ_{MMF} in Fig. 7; this is the same as the aforementioned theoretical predictions evaluated to linear order in χ_L [14,32]. The theory for $\overline{\tau}(\mathrm{on})$ approaches the simulation results with increasing α due to the field-particle interaction becoming dominant, and the same asymptotic behavior being reached as with noninteracting particles. The theory for $\overline{\tau}(\mathrm{off})$ shows a small hump in the region of $\alpha = 5$, but then approaches $5\tau_B/4$ as per Eq. (55). Overall, the theory and simulations are in good qualitative agreement, with the difference in apparent timescales being comparable to the error in evaluating the limiting theoretical values [Eqs. (48) and (54)] to linear order in χ_L.

The magnetization growth in systems with $\chi_L = 2$ is shown in Fig. 8. The picture is the same as before, with there being good agreement between theory and simulation with very small and vary large values of α, but in between, the theory overestimates the growth rate. This overestimation is much more pronounced than with $\chi_L = 1$.

Similarly, the instantaneous growth times $\tau(t)$ shown in Fig. 4(b) follow the same kinds of trends as with $\chi_L = 1$, but the predicted differences between interacting and noninteracting systems are obviously larger. The deviation between the theory and the small number of simulation results is also significant.

The average growth and relaxation times in systems with $\chi_L = 2$ are shown in Fig. 9. The same picture emerges as with the weaker interactions, except that the deviations between theory and simulation are larger. From theory, in the weak-field limit, $\overline{\tau}(\mathrm{on}) = \overline{\tau}(\mathrm{off}) = 7\tau_B/5$ [Eqs. (48) and (54)], and in the strong-field limit, $\overline{\tau}(\mathrm{off}) = 3\tau_B/2$ (55). The theoretical relationship between the values of $\overline{\tau}(\mathrm{off})$ in these two limits is not reflected in the simulation results, and therefore, this could be a mathematical artifact. The linearized approximation of Eq. (54) is closer to the simulation results.

IV. CONCLUSIONS

The dynamics of magnetization growth and relaxation in ferrofluids were studied using theory and Brownian-dynamics simulations. Growth occurs when an applied field is switched on, and relaxation occurs when an applied field is switch off. The theoretical approach is based on solving the Fokker-Planck-Brown equation for a single particle, with an approximate "modified mean-field" treatment of interactions based on an additional field arising from the magnetization of the other particles. The particle dynamics were restricted to Brownian rotations. For noninteracting particles, the theory matches essentially exactly with the simulations. With weak fields, the average growth and relaxation times are the same, and equal to the Brownian rotation time. The average growth time decreases rapidly with increasing field due to the extra torque acting on the particles, while the average relaxation time remains constant at its Brownian value. Including interactions increases the average growth and relaxation times with weak fields, but the changes are less significant with increasing field, because the field-particle interactions dominate the particle-particle interactions. The agreement between theory and simulation is qualitative. The theory also provides insights on the evolution of the dynamics during the growth and relaxation processes, but it is difficult to test those predictions because of statistical noise in the simulation results.

As noted before in applications of the modified mean-field approach to equilibrium and nonequilibrium dynamics [14,17], the predictions are only accurate to first order in the Langevin susceptibility. Moreover, there can also be some characteristic artifacts in the associated dynamical functions such as the magnetization relaxation curve $m(t)$. In earlier work, it was found that related approaches based on the Weiss mean-field theory can provide much more accurate predictions [15,17]. Unfortunately, it has not yet been possible to adapt Weiss-like approaches to the current problem of magnetization growth dynamics, but hopefully this can be resolved soon. This might extend the range of validity of theoretical predictions to include moderately strong interactions, meaning larger values of χ_L. It would also be interesting to examine the magnetization growth dynamics in strongly interacting systems, where chain and ring formation can occur [43].

Finally, this study has been restricted to monodisperse ferrofluids, although the magnetization relaxation in polydisperse ferrofluids has been tackled before [19]. This should also be possible for magnetization growth because the fundamental principles are understood, and it is just a case of applying the methods to model systems that are representative of real ferrofluids.

ACKNOWLEDGMENTS

The research of A.O.I. and I.M.S. was partially supported by the Ural Mathematical Center within Project No. 075-02-2024-1428. P.J.C. thanks Patrick Ilg (University of Reading) for helpful comments on the work.

[1] R. E. Rosensweig, *Ferrohydrodynamics* (Dover Publications, Mineola, NY, 1998).
[2] B. F. Edwards, D. M. Riffe, J.-Y. Ji, and W. A. Booth, Interactions between uniformly magnetized spheres, Am. J. Phys. **85**, 130 (2017).
[3] S. Odenbach and S. Thurm, Magnetoviscous effects in ferrofluids, in *Ferrofluids: Magnetically Controllable Fluids and Their Applications*, edited by S. Odenbach (Springer, Berlin, 2002), pp. 185–201.
[4] J. Philip and J. M. Laskar, Optical properties and applications of ferrofluids—A review, J. Nanofluids **1**, 3 (2012).
[5] A. O. Ivanov and P. J. Camp, How particle interactions and clustering affect the dynamic magnetic susceptibility of ferrofluids, J. Magn. Magn. Mater. **586**, 171216 (2023).
[6] K. Everaert, D. Eberbeck, R. Korber, P. Radon, B. Van Waeyenberge, J. Leliaert, and F. Wiekhorst, Comparing magnetization fluctuations and dissipation in suspended magnetic nanoparticle ensembles, IEEE Trans. Magn. (2024), doi:10.1109/TMAG.2024.3424275.
[7] J. Lange, R. Kötitz, A. Haller, L. Trahms, W. Semmler, and W. Weitschies, Magnetorelaxometry–a new binding specific detection method based on magnetic nanoparticles, J. Magn. Magn. Mater. **252**, 381 (2002).
[8] F. Ludwig, S. Mäuselein, E. Heim, and M. Schilling, Magnetorelaxometry of magnetic nanoparticles in magnetically unshielded environment utilizing a differential fluxgate arrangement, Rev. Sci. Instrum. **76**, 106102 (2005).
[9] D. Eberbeck, F. Wiekhorst, U. Steinhoff, and L. Trahms, Aggregation behaviour of magnetic nanoparticle suspensions investigated by magnetorelaxometry, J. Phys.: Condens. Matter **18**, S2829 (2006).
[10] F. Ludwig and H. Remmer, Rotational dynamics of magnetic nanoparticles in different matrix systems, Phys. Sci. Rev. **7**, 981 (2022).
[11] F. Wiekhorst, U. Steinhoff, D. Eberbeck, and L. Trahms, Magnetorelaxometry assisting biomedical applications of magnetic nanoparticles, Pharm. Res. **29**, 1189 (2012).
[12] M. Liebl, F. Wiekhorst, D. Eberbeck, P. Radon, D. Gutkelch, D. Baumgarten, U. Steinhoff, and L. Trahms, Magnetorelaxometry procedures for quantitative imaging and characterization of magnetic nanoparticles in biomedical applications, Biomed. Eng.-Biomed. Tech. **60**, 427 (2015).
[13] T. Vangijzegem, D. Stanicki, A. Panepinto, V. Socoliuc, L. Vekas, R. N. Muller, and S. Laurent, Influence of experimental parameters of a continuous flow process on the properties of very small iron oxide nanoparticles (VSION) designed for T_1-weighted magnetic resonance imaging (MRI), Nanomaterials **10**, 757 (2020).
[14] J. O. Sindt, P. J. Camp, S. S. Kantorovich, E. A. Elfimova, and A. O. Ivanov, Influence of dipolar interactions on the magnetic susceptibility spectra of ferrofluids, Phys. Rev. E **93**, 063117 (2016).
[15] A. O. Ivanov and P. J. Camp, Theory of the dynamic magnetic susceptibility of ferrofluids, Phys. Rev. E **98**, 050602(R) (2018).
[16] T. M. Batrudinov, Y. E. Nekhoroshkova, E. I. Paramonov, V. S. Zverev, E. A. Elfimova, A. O. Ivanov, and P. J. Camp, Dynamic magnetic response of a ferrofluid in a static uniform magnetic field, Phys. Rev. E **98**, 052602 (2018).
[17] A. O. Ivanov and P. J. Camp, Effects of interactions on magnetization relaxation dynamics in ferrofluids, Phys. Rev. E **102**, 032610 (2020).
[18] A. O. Ivanov and P. J. Camp, Effects of interactions, structure formation, and polydispersity on the dynamic magnetic susceptibility and magnetic relaxation of ferrofluids, J. Mol. Liq. **356**, 119034 (2022).
[19] A. O. Ivanov and P. J. Camp, Magnetization relaxation dynamics in polydisperse ferrofluids, Phys. Rev. E **107**, 034604 (2023).
[20] P. Ilg and M. Kröger, Dynamics of interacting magnetic nanoparticles: Effective behavior from competition between Brownian and Néel relaxation, Phys. Chem. Chem. Phys. **22**, 22244 (2020).
[21] P. Ilg and M. Kröger, Field- and concentration-dependent relaxation of magnetic nanoparticles and optimality conditions for magnetic fluid hyperthermia, Sci. Rep. **13**, 16523 (2023).
[22] P. Ilg, Nonequilibrium response of magnetic nanoparticles to time-varying magnetic fields: Contributions from Brownian and Néel processes, Phys. Rev. E **109**, 034603 (2024).
[23] I. S. Poperechny, Multipeak dynamic magnetic susceptibility of a superparamagnetic nanoparticle suspended in a fluid, Phys. Rev. B **107**, 064416 (2023).
[24] I. S. Poperechny, Superparamagnetic effects in the linear magnetic response of polydisperse ensembles of nanoparticles suspended in a fluid, Phys. Rev. E **109**, 044601 (2024).
[25] T. Yoshida and K. Enpuku, Simulation and quantitative clarification of AC susceptibility of magnetic fluid in nonlinear Brownian relaxation region, Jpn. J. Appl. Phys. **48**, 127002 (2009).
[26] W. F. Brown, Jr., Thermal fluctuations of a single-domain particle, J. Appl. Phys. **34**, 1319 (1963).

[27] W. F. Brown, Jr., Thermal fluctuations of a single-domain particle, Phys. Rev. **130**, 1677 (1963).

[28] W. F. Brown, Jr., Thermal fluctuation of fine ferromagnetic particles, IEEE Trans. Magn. **15**, 1196 (1979).

[29] Y. R. Chemla, H. L. Grossman, T. S. Lee, J. Clarke, M. Adamkiewicz, and B. B. Buchanan, A new study of bacterial motion: Superconducting quantum interference device microscopy of magnetotactic bacteria, Biophys. J. **76**, 3323 (1999).

[30] A. O. Ivanov and O. B. Kuznetsova, Magnetic properties of dense ferrofluids: An influence of interparticle correlations, Phys. Rev. E **64**, 041405 (2001).

[31] A. O. Ivanov, V. S. Zverev, and S. S. Kantorovich, Revealing the signature of dipolar interactions in dynamic spectra of polydisperse magnetic nanoparticles, Soft Matter **12**, 3507 (2016).

[32] A. Y. Zubarev and A. V. Yushkov, Dynamic properties of moderately concentrated magnetic liquids, J. Exp. Theor. Phys. **87**, 484 (1998).

[33] B. U. Felderhof and R. B. Jones, Mean field theory of the nonlinear response of an interacting dipolar system with rotational diffusion to an oscillating field, J. Phys.: Condens. Matter **15**, 4011 (2003).

[34] M. S. Rusanov, V. S. Zverev, and E. A. Elfimova, Dynamic magnetic susceptibility of a ferrofluid: The influence of interparticle interactions and ac field amplitude, Phys. Rev. E **104**, 044604 (2021).

[35] A. O. Ivanov, S. S. Kantorovich, E. N. Reznikov, C. Holm, A. F. Pshenichnikov, A. V. Lebedev, A. Chremos, and P. J. Camp, Magnetic properties of polydisperse ferrofluids: A critical comparison between experiment, theory, and computer simulation, Phys. Rev. E **75**, 061405 (2007).

[36] W. T. Coffey and Y. P. Kalmykov, *The Langevin Equation: With Applications to Stochastic Problems in Physics, Chemistry and Electrical Engineering*, 3rd ed., World Scientific Series in Contemporary Chemical Physics, Vol. 27 (World Scientific, Singapore, 2012).

[37] M. Tenenbaum and H. Pollard, *Ordinary Differential Equations*, Dover Books on Mathematics (Dover Publications, Mineola, NY, 1986).

[38] LAMMPS Molecular Dynamics Simulator, https://www.lammps.org/ (2024).

[39] A. P. Thompson, H. M. Aktulga, R. Berger, D. S. Bolintineanu, W. M. Brown, P. S. Crozier, P. J. in 't Veld, A. Kohlmeyer, S. G. Moore, T. D. Nguyen, R. Shan, M. J. Stevens, J. Tranchida, C. Trott, and S. J. Plimpton, LAMMPS—A flexible simulation tool for particle-based materials modeling at the atomic, meso, and continuum scales, Comput. Phys. Commun. **271**, 108171 (2022).

[40] J. D. Weeks, D. Chandler, and H. C. Andersen, Role of repulsive forces in determining the equilibrium structure of simple liquids, J. Chem. Phys. **54**, 5237 (1971).

[41] M. A. Martsenyuk, Y. L. Raikher, and M. I. Shliomis, On the kinetics of magnetization of suspensions of ferromagnetic particles, Sov. Phys. JETP **38**, 413 (1974).

[42] M. I. Shliomis and Y. L. Raikher, Experimental investigations of magnetic fluids, IEEE Trans. Magn. **16**, 237 (1980).

[43] P. J. Camp, A. O. Ivanov, and J. O. Sindt, How chains and rings affect the dynamic magnetic susceptibility of a highly clustered ferrofluid, Phys. Rev. E **103**, 062611 (2021).